



# **iJRASET**

International Journal For Research in  
Applied Science and Engineering Technology



---

# **INTERNATIONAL JOURNAL FOR RESEARCH**

IN APPLIED SCIENCE & ENGINEERING TECHNOLOGY

---

**Volume: 5      Issue: VII      Month of publication: July 2017**

**DOI:**

**[www.ijraset.com](http://www.ijraset.com)**

**Call: ☎ 08813907089**

**E-mail ID: [ijraset@gmail.com](mailto:ijraset@gmail.com)**

# Enhancement of Photocatalytic Activity by $\text{Mg}^{2+}$ Doped Ceria Quantum Dots

V. Ramasamy<sup>1</sup>, V. Mohana<sup>2</sup>

<sup>1,2</sup>Department of Physics, Annamalai University, Annamalai Nagar, 608 002, INDIA

**Abstract:** The pure and  $\text{Mg}^{2+}$  doped  $\text{CeO}_2$  quantum dot were synthesized by sol-gel technique. The prepared quantum dots were characterized using X-ray diffraction pattern (XRD), Scanning electron microscope (SEM-EDX). The XRD results show cubic structure of the  $\text{CeO}_2$  quantum dots. The crystalline size ( $D$ ), microstrain ( $\epsilon$ ), dislocation density ( $\delta$ ) and lattice parameter ( $a$ ) were calculated and analyzed. SEM-EDX analysis shows the morphology and the presence of elements. The photocatalytic activity of the synthesized quantum dot was evaluated based on the photodegradation of methylene blue (MB) by UV-Vis spectrometry.

**Key Words:** Quantum dot, Sol-gel, cubic, UV-visible, photocatalytic, methylene blue.

## I. INTRODUCTION

In the sustainable development of human society, environmental pollution is becoming the topic of prime issue. The photocatalysis process has drawn much attention since it has potential solution to the energy production and wastewater cleaning. Now a days, semiconductor photocatalysis has attracted increasing interest due to its degradation capability of organic pollutants [1]. The inefficient use of solar energy and the rapid charge recombination largely limit its practical application. Hence, much research activities has been devoted to improve the solar energy conversion efficiency and enhance the photocatalytic activity by modifying the exiting photocatalysts [2]. The discharges of dyes having higher stability in to water, from textile industries are harmful to humans and animals. Normally, dyes are double bonded different chromopheric groups, and heterocyclic graph which absorb visible light. The reduction of the chromopheric group shifts the visible region to the UV or IR region. Hence, a reduction in color can be achieved. In recent years, heterogeneous photocatalytic oxidation has received considerable attention for removing the dyes in textile effluents. Dyes can also inhibit sunlight into streams and affect the photosynthetic reactions. Methylene blue (MB) is one of the most commonly used substances for cotton, coloring, paper stocks, wood and silk. It is also utilized in medicine as well. The continuous exposure to MB will cause increased heart rate, vomiting, shock, Heinz body formation, jaundice, cyanosis and quadriplegia, and tissue necrosis in humans [3]. Nanoparticles with their large surface area to volume ratio have been studied to propose them as candidates for photocatalytic agents.

Materials based on cerium is the most abundant among the rare earth elements. It occupies 0.0046 wt% of the Earth's crust. The applications of cerium has become more and more widespread, sunscreen for ultraviolet absorbents [4], solid oxide fuel cells [5], solar cells, water purification [6], oxygen storage capacity [7] and optical devices [8]. Metal oxides of cerium has a fluorite-like cubic structure in which each cerium site is surrounded by eight oxygen sites in face-centered cubic (FCC) arrangement. Each oxygen site has a tetrahedron cerium site. Several chemical methods can be used for the synthesis of pure or doped  $\text{CeO}_2$  [9].

In the present study, the sol gel method is employed to prepare pure and  $\text{Mg}^{2+}$  doped  $\text{CeO}_2$  quantum dots. The structural, morphological, elemental and photocatalytic analysis of the ceria quantum dots were analyzed using X-ray powder diffraction (XRD) and Scanning electron microscope (SEM-EDX). The photocatalytic activity of  $\text{Mg}^{2+}:\text{CeO}_2$  quantum dots using methylene blue (MB) dye was also analyzed using UV-Vis spectrometry.

## II. EXPERIMENTAL TECHNIQUES

### A. Materials

Cerium (IV) nitrate  $(\text{NH}_4)_2[\text{Ce}(\text{NO}_3)_6]$  from Nice Chemical company, Ammonium hydroxide ( $\text{NH}_3$ ) obtained from spectrum reagents and chemicals Pvt. Ltd, Citric acid anhydrous ( $\text{C}_6\text{H}_8\text{O}_7$ ) obtained from s-d Fine Chem. Ltd, and deionized water (DI) were used to synthesize pure and  $\text{Mg}^{2+}$  doped  $\text{CeO}_2$  quantum dots. The purity of the chemicals were above 99%. For all dilution and sample preparation ultrapure water was used. In all the experimental work, acid washed glass wares were used.

### B. Methods

The  $Mg^{2+}$  doped  $CeO_2$  quantum dots were synthesized using sol-gel method. In a typical procedure, 5.2g (0.4M) of Cerium (IV) nitrate  $(NH_4)_2[Ce(NO_3)_6]$  in 25ml of deionized water aqueous mixed with Magnesium acetate (0.1, 0.3, 0.5 and 0.7 M.%) in 25ml of deionized water under constant stirring. The saturated solution of citric acid was added drop wise in to the mixture. After these,  $NH_3$  was added to the precursor solution in order to maintain the pH of the solution. The clear solution was completely turned to a gel after continuous stirring for 4 hours at  $70^\circ C$ . Then, the gel was dried and ground into powder. The product was calcined at different temperatures from 200-700  $^\circ C$  in steps of 100  $^\circ C$  using muffle furnace. However, the samples calcined at 400  $^\circ C$  shows higher crystallinity then others. This was tested through XRD analysis.

### C. Photocatalytic Activity

The photocatalytic activity of pure and  $Mg^{2+}$  doped  $CeO_2$  quantum dots was evaluated by performing methylene blue (MB) degradation reactions under open air sunlight irradiation. In an experiment, 100ml of  $5 \times 10^{-3}$  M aqueous MB solution and 0.2 g of fine powder catalyst were taken. The suspensions were magnetically stirred in the dark for 30 min to attain adsorption-desorption equilibrium between the dye and pure and  $Mg^{2+}$  doped  $CeO_2$  quantum dots. During the illumination time, no volatility of the solvent was observed. Then it was continuously stirred. The aliquots of the reaction mixture were collected at regular time intervals (10 min) and centrifuged. Then the concentration of dye in the residual solution was studied using a UV-1650 PC SHIMADZU spectrometer. The period is ranging from 0 to 50 min. The sample aliquots were withdrawn from the reaction mixture at a regular time interval. Changes in the concentration of MB were observed from its characteristic absorption maxima at 663 nm.

### D. Characterization of Sol-Gel Derived $CeO_2$ Quantum Dots

Using X pert PRO diffractometer with a Cu  $K\alpha$  radiation ( $K\alpha = 1.5406 \text{ \AA}$ ), the X-ray diffraction (XRD) patterns of the powdered samples were recorded. The morphological studies of the products were analyzed using scanning electron microscopy. These measurements were performed on a JEOL- 6610 scanning electron microscope. Energy-dispersive X-ray analysis (EDX) measurement was carried out using Bruker 129 eV, to get elemental composition (%). Before the measurement, the samples were mounted on copper stubs by double sided carbon tapes and the gold is coated using the sputtering technique. The optical absorption spectra of the samples were recorded by UV-1650 PC SHIMADZU spectrometer.

## III. RESULTS AND DISCUSSION

### A. X-Ray Diffraction Study

Figure.1 gives the XRD patterns of the pure and  $Mg^{2+}$  (0.1, 0.3, 0.5 and 0.7 M.%) doped  $CeO_2$  nanoparticles. The observed planes such as (111), (200), (220), (311), (222), (400) and (331) are consistent with the cubic structure of  $CeO_2$  in the standard data from the Joint Commutee on Powder Diffraction Standards (JCPDS: 34-0394).

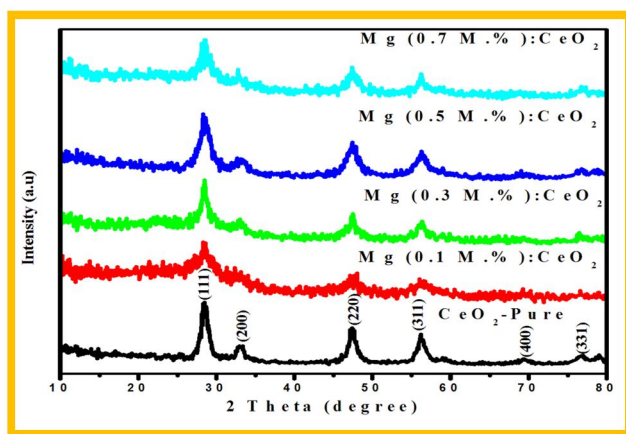


Figure 1: X-ray diffraction patterns of pure and  $Mg^{2+}$  (0.1, 0.3, 0.5 and 0.7 M.%) doped  $CeO_2$  quantum dots.

### B. Crystalline Size

The average crystallite size was calculated using Debye-Scherrer's formula [10].

$$D_{XRD} = \frac{K\lambda}{\beta \cos \theta} \quad (1)$$

Where,  $D$  is crystallite size,  $\beta$  is full width of half maximum (FWHM),  $K$  is factor ( $K=0.9$  in this work),  $\lambda$  is the wavelength of incident X-rays ( $\lambda = 0.15406\text{nm}$ ). The crystallite size of the pure and  $\text{Mg}^{2+}$  (0.1, 0.3, 0.5 and 0.7 M.%) doped  $\text{CeO}_2$  quantum dots are in the range 10.98 to 16.66 nm (Table 1). The typical size of the particles is less compared to twice the value of the exciton Bohr radius of the  $\text{CeO}_2$  (7-8 nm) [11]. Hence the obtained product is called of quantum dot. The increasing of 0.1 M.% ( $\text{Mg}^{2+}$ ) concentration express decrease the crystallite size. Moreover, it can be observed that doping of  $\text{Mg}^{2+}$  with  $\text{CeO}_2$  can hinder the crystal growth of the crystal and this favors the observance of decreasing crystallite sizes [12].

Sample name	Lattice parameter (a) nm		Dislocation density( $\delta$ ) $\times 10^{16}$	Micro strain ( $\epsilon$ ) $\times 10^{-3}$	Particle size
	For bulk	For nano			Scherrer's formula
$\text{CeO}_2$ -Pure	0.5411	0.5450	8.29	2.9105	10.98
$\text{Mg}(0.1 \text{ M.}): \text{CeO}_2$	-	0.5435	0.02	2.0794	6.94
$\text{Mg}(0.3 \text{ M.}): \text{CeO}_2$	-	0.5408	3.60	4.9781	16.66
$\text{Mg}(0.5 \text{ M.}): \text{CeO}_2$	-	0.5418	5.18	3.3265	13.89
$\text{Mg}(0.7 \text{ M.}): \text{CeO}_2$	-	0.5427	9.21	2.4951	10.42

Table 1: Different parameters of pure and Mg-doped  $\text{CeO}_2$  quantum dots from XRD

### C. Lattice Parameter (a)

The lattice parameter of undoped and  $\text{Mg}^{2+}$  doped  $\text{CeO}_2$  quantum dots are calculated by the Eq. 2 [13].

$$a = \frac{n\lambda}{2\sin\theta} \sqrt{h^2 + k^2 + l^2} \quad (2)$$

Where,  $\lambda$  is the wavelength of incident X-rays ( $\lambda = 0.15406 \text{ nm}$ ),  $hkl$  are the Miller indices. The calculated values shows that lattice parameter of  $\text{Mg}^{2+}$  (0.1 M.%) doped  $\text{CeO}_2$  is 0.5435 nm which is less than that of bulk  $\text{CeO}_2$  (0.5411 nm) [14]. This may be due to the substitution of smaller  $\text{Mg}^{2+}$  (ionic radius =  $0.72\text{\AA}$ ) by the bigger  $\text{Ce}^{4+}$  (ionic radius =  $0.97\text{\AA}$ ) which is supposed to reduced inter atomic spacing. Hence the reduction in lattice parameter is expected with  $\text{Mg}^{2+}$  doping [15].

### D. Microstrain ( $\epsilon$ ) and Dislocation Density ( $\delta$ )

The Microstrain ( $\epsilon$ ) and Dislocation density ( $\delta$ ) are calculated by following Eq. 3 and 4 [16].

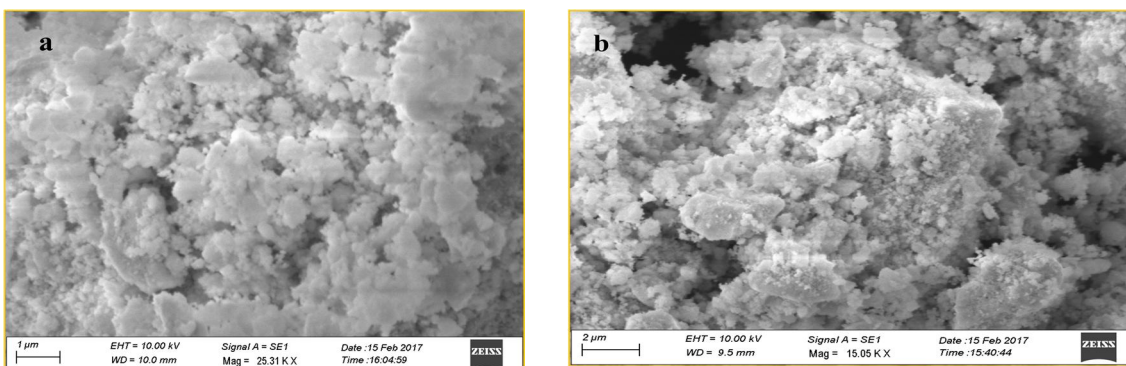
$$\epsilon = \frac{\beta \cos \theta}{4} \quad (3)$$

$$\delta = \frac{1}{D^2} \quad (4)$$

Where,  $D$  crystalline size,  $\theta$  is Bragg angle and  $\beta$  is the full width of half maximum (FWHM). The values are tabulated in Table 1. From this, it is observed that the dislocation density and microstrain increases with decreasing in particle size. According to Erwin et al [17], if the formation energy of the quantum dots is very high, the impurity will be expelled from the cluster and incorporation should be expected just for larger nanocrystals. The decrease in dislocation density, micro strain and stacking fault improved the crystallinity of the sample [16].

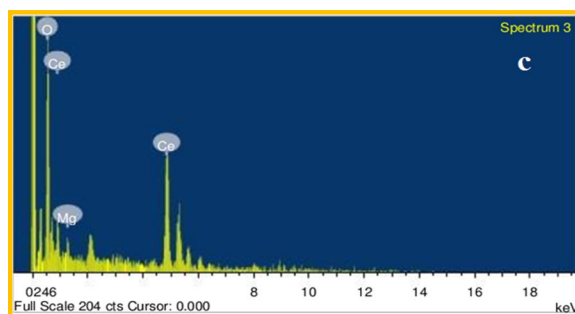


### E. Scanning Electron Microscopy (SEM)



The morphology of the pure and  $Mg^{2+}$  doped  $CeO_2$  quantum dots have been characterized by SEM analyses which are shown in Fig. 2 (a-b).

Figure 2: SEM image of (a) pure  $CeO_2$  and (b) doped with  $Mg^{2+}$  (0.1 M.%) quantum dots (c) EDX



Figures 3: percentage (a) degradation and (b) decolorization of pure and  $Mg^{2+}$  (0.1, 0.3, 0.5 and 0.7 M.%) doped  $CeO_2$  quantum dots.

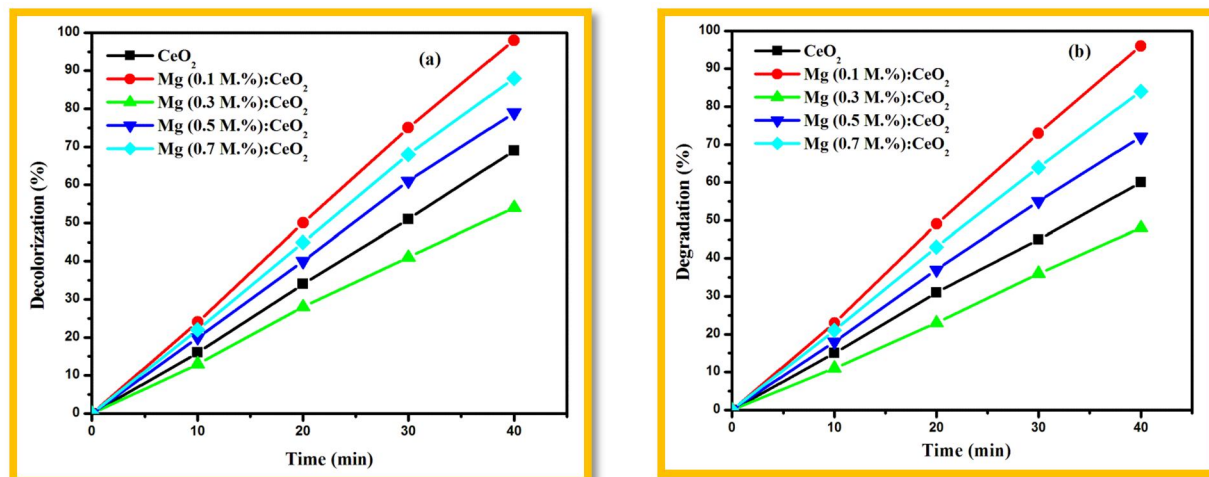
The SEM images of pure particles consist of non-uniform distribution with some single particles or with some clustered particles. The  $Mg^{2+}$  (0.1 M.%) doped  $CeO_2$  quantum dots show better distribution particles compared to pure  $CeO_2$  quantum dots. This confirms the influence of  $Mg^{2+}$  doped in ceria. Figure 2 (c) shows the energy dispersive X-ray (EDX) spectrum which confirms the presence of Ce, O and Mg.

### F. Photocatalytic Efficiency of $CeO_2$ Quantum Dots

The photocatalytic efficiency of pure and  $Mg^{2+}$  (0.1, 0.3, 0.5 and 0.7 M.%) doped  $CeO_2$  quantum dots was studied under open air sunlight irradiation. The photocatalytic efficiency was recorded in UV-Visible spectroscopy from 200 to 800 nm. The intensity of strong absorption band of MB located at  $\lambda = 663$  nm decrease gradually with respect to increasing irradiation time. The absorbance of MB was nearly zero after 50 min of nature sun light using pure and  $Mg^{2+}$  doped  $CeO_2$  quantum dots. The change in absorbance was measured at an interval of 10 minutes for a period of 50 minutes (5 cycles).

Table 2: Total percentage degradation and decolorization of pure and Mg doped  $CeO_2$  quantum dots.

S. No	Samples	Degradation (%)	Decolorization (%)	Crystalline size (D) from XRD
1	$CeO_2$ -pure	61	69	10.98
2	Mg (0.1 M.%) : $CeO_2$	96	98	6.94
3	Mg (0.3 M.%) : $CeO_2$	48	54	16.66
4	Mg (0.5 M.%) : $CeO_2$	72	79	13.89
5	Mg (0.7 M.%) : $CeO_2$	84	88	10.42



The photodegradation and decolorization efficiency (%D) of the materials in the MB are calculated using the following expression.

$$\%D = \frac{C_0 - C_t}{C_0} \times 100 \quad (5)$$

$$\%D = 100(A_i - A_t)/A_i \quad (6)$$

Where, D is the degradation and decolorization of the dye (%),  $C_0$ ,  $A_i$  is the initial concentration of MB and  $C_t$ ,  $A_t$  is the remaining concentration of MB after irradiation in the desired time interval [18, 19].

Figure 3 (a & b) shows the photodegradation and decolorization of pure and  $Mg^{2+}$  (0.1, 0.3, 0.5 and 0.7 M.%) doped  $CeO_2$  quantum dots under open air sun light irradiation. The calculated values are shown in Table 2. It can be seen that the photocatalytic activity of the  $Mg^{2+}$  (0.1 M.%): $CeO_2$  quantum dots is maximum compared to 0.3, 0.5 and 0.7 M.% ( $Mg^{2+}$ ) doped  $CeO_2$  quantum dots. Based on above, it can be concluded that  $Mg^{2+}$  (0.1 M.%):  $CeO_2$  sample acts as a good photocatalyst towards the degradation and decolorization of MB. Also MB have a greater affinity toward the catalyst, resulting in a much higher removal capacity. These results confirmed that the synthesized  $Mg^{2+}$ : $CeO_2$  quantum dots exhibited excellent catalytic activity. According to R. Marshall [20], the overall photocatalytic reaction involves three major steps: (i) absorption of light by a semiconductor to generate electron-hole pairs, (ii) charge separation and migration to the surface of the semiconductor, and (iii) the reactant adsorption and surface reactions. Based on the results, the enhanced photocatalytic activities of  $Mg^{2+}$  (0.1 M.%) doped  $CeO_2$  can be partially attributed to the smaller particle size and the highly reactive facets exposed.

#### IV. CONCLUSION

The pure and  $Mg^{2+}$  doped ceria quantum dots were successfully synthesized by sol - gel method. The formation of face-centered cubic structures with small crystallites sizes are in the range 10-16 nm by XRD analysis. The formation of less agglomerated particles with spherical shapes, are studied through SEM with EDX. A better performance of photocatalytic activity was found to 50 min irradiation time for  $Mg^{2+}$  doped  $CeO_2$  quantum dots. Thus, it is concluded that the synthesized  $Mg^{2+}$ :  $CeO_2$  quantum dots are one of the best candidates for environmental applications as a photocatalyst.

#### REFERENCES

- [1] Chaisorn J, Wetchakun K, Phanichphant S and Wetchakun N., 2015. A novel  $CeO_2$  /InVO 4 composite with high visible-light induced photocatalytic activity, Mater Let, 160, 75–80.
- [2] Zhang J, Yu J, Jaroniec M and Gong J. R., 2012. Noble Metal-Free Reduced Graphene Oxide-ZnxCd1-xS Nanocomposite with Enhanced Solar Photocatalytic  $H_2$  Production Performance, Nano Letters, 12(9), 4584–4589.
- [3] Nezamzadeh-Ejhi A and Zabihi-Mobarakeh H., 2014. Heterogeneous photodecolorization of mixture of methylene blue and bromophenol blue using CuO-nano-clinoptilolite, J Ind Eng Chem, 20(4), 1421–1431.
- [4] Kakuta N, Morishima N, Kotobuki M, Iwase T, Mizushima T, Sato Y and Matsuura S., 1997. Oxygen storage capacity (OSC) of aged Pt/ $CeO_2$ /Al $_2$ O $_3$  catalysts: roles of Pt and  $CeO_2$  supported on Al $_2$ O $_3$ , Appl Surf Sci, 121–122, 408–412.
- [5] Yahiro H., 1988. High Temperature Fuel Cell with Ceria-Yttria Solid Electrolyte, J Electrochem Soc., 135(8), 2077.

- [6] Ji P, Zhang J, Chen F and Anpo M., 2009. Study of adsorption and degradation of acid orange 7 on the surface of CeO<sub>2</sub> under visible light irradiation, *Appl Catal B*, 85(3–4), 148–154.
- [7] Lira-Cantu M and Krebs F. C., 2006. Hybrid solar cells based on MEH-PPV and thin film semiconductor oxides (TiO<sub>2</sub>, Nb<sub>2</sub>O<sub>5</sub>, ZnO, CeO<sub>2</sub> and CeO<sub>2</sub>-TiO<sub>2</sub>): Performance improvement during long-time irradiation, *Sol Energ Mat Sol Cells*, 90(14), 2076–2086.
- [8] Kanakaraju S, Mohan S and Sood A. K., 1997. Optical and structural properties of reactive ion beam sputter deposited CeO<sub>2</sub> films, *Thin Solid Films*, 305(1–2), 191–195.
- [9] Kumar E, Selvarajan P and Muthuraj D., 2013. Synthesis and characterization of CeO<sub>2</sub> nanocrystals by solvothermal route, *Mat Res*, 16(2), 269–276.
- [10] Cullity B. D., 1978. Reading: Addition –Wesley pub.
- [11] Renuka N. K, Harsha N and Divya T., 2015. Supercharged ceria quantum dots with exceptionally high oxygen buffer action, *RSC Adv*, 49, 38837–38841.
- [12] Channei D, Inceesungvorn B, Wetchakun N, Phanichphant S, Nakaruk A, Koshy P and Sorrell C. C., 2013. Photocatalytic activity under visible light of Fe-doped CeO<sub>2</sub> nanoparticles synthesized by flame spray pyrolysis, *Ceram Int*, 39(3), 3129–3134.
- [13] Ramasamy V and Vijayalakshmi G., 2015. Effect of Zn doping on structural, optical and thermal properties of CeO<sub>2</sub> nanoparticles, *Superlattices Microstruct*, 85, 510–521.
- [14] Taniguchi T, Watanabe T, Sakamoto N, Matsushita N and Yoshimura M., 2008. Aqueous Route to Size-Controlled and Doped Organophilic Ceria Nanocrystals, *Cryst Growth Des*, 8(10), 3725–3730.
- [15] Alla S. K, Mandal R. K and Prasad N. K., 2016. Optical and magnetic properties of Mg<sup>2+</sup> doped CeO<sub>2</sub> nanoparticles, *RSC Adv*, 6(105), 103491–103498.
- [16] Suresh R, Ponnuswamy V and Mariappan R., 2013. Effect of annealing temperature on the microstructural optical and electrical properties of CeO<sub>2</sub> nanoparticles by chemical precipitation method, *Appl Surf Sci*, 273, 457–464.
- [17] Erwin S. C, Zu L, Haftel M. I, Efros A. L and Kennedy T. A., 2005. Doping semiconductor nanocrystals, *Nature*, 436 (7047), 91–94.
- [18] Sifontes A. B, Rosales M, Méndez F. J, Oviedo O and Zoltan T., 2013. Effect of Calcination Temperature on Structural Properties and Photocatalytic Activity of Ceria Nanoparticles Synthesized Employing Chitosan as Template, *J Nanomater*, 1–9.
- [19] Rajendran R, Karthik Sundaram S, Yasodha K and Umamaheswari K., 2012. Comparison of fungal laccase production on different solid Substrates immobilization and its decolorization potential on synthetic textile dyes, *Iioabj*, 3 (5), 1–6.
- [20] Marschall R., 2013. Semiconductor Composites: Strategies for Enhancing Charge Carrier Separation to Improve Photocatalytic Activity, *Adv Funct Mater*, 24(17), 2421–2440.





10.22214/IJRASET



45.98



IMPACT FACTOR:  
7.129



IMPACT FACTOR:  
7.429



# INTERNATIONAL JOURNAL FOR RESEARCH

IN APPLIED SCIENCE & ENGINEERING TECHNOLOGY

Call : 08813907089  (24\*7 Support on Whatsapp)